Ilvaite from a serpentinized peridotite in the Asama igneous complex, Mikabu greenstone belt, Sambagawa metamorphic terrain, central Japan

TAKASHI AGATA AND MAMORU ADACHI

Department of Earth and Planetary Sciences, Nagoya University, Nagoya, 464-01 Japan

Abstract

Ilvaite is sparsely disseminated in a serpentinized plagioclase wehrlite of the Asama igneous complex that underwent the Sambagawa regional metamorphism of pumpellyite–actinolite to greenschist facies. Ilvaite in the Asama complex is monoclinic (a = 13.019(5), b = 8.808(2), c = 5.850(4) Å, β = 90.19(4)°), and its composition is similar to the ideal end-member composition ($CaFe_2^{2+}Fe^{3+}Si_2O_8OH$). Ilvaite occurs in mats of serpentine (chrysotile); it probably formed during serpentinization, which might have accompanied the Sambagawa metamorphism. The associated secondary minerals include salitic clinopyroxene, magnetite and andradite. The ilvaite-free mineral assemblage that formed during the serpentinization is usually serpentine–clinopyroxene–magnetite, which is widespread in the complex. The phase relations between coexisting minerals suggest that the conditions during the formation of the ilvaite-bearing assemblage were reducing when compared to those of the assemblage serpentine–clinopyroxene–magnetite. The reducing conditions during the ilvaite formation were presumably brought about by hydrogen gas that1 was generated during the serpentinization of olivine.

KEYWORDS: ilvaite, serpentinization, reducing conditions, Asama igneous complex, Mikabu greenstone belt, Sambagawa metamorphism.

Introduction

ILVAITE is a rather rare Ca-Fe silicate, and typically occurs in Ca–Fe–Si skarn (Burt, 1971; Pesquera and Velasco, 1986). Ilvaite has been reported as a hydrothermal product in the upper part of the Skaergaard intrusion (Ramdohr, 1969; Naslund *et al.*, 1983) and in a dolerite dyke in Norway (Barton and Bergen, 1984). It also occurs in rodingites associated with serpentinite (Lucchetti, 1989) and in Fe-rich veins cutting metamorphosed serpentinite (Dietrich, 1972; Graeser, 1975).

Ilvaite is sparsely disseminated in a serpentinized peridotite of the Asama igneous complex, a layered mafic–ultramafic intrusion in the Mikabu greenstone belt, Mie Prefecture, central Japan (Agata, 1989, 1994). It is associated with serpentine, secondary salitic clinopyroxene, magnetite and andradite. This paper describes the occurrence, mineral paragenesis, and physical and chemical properties of ilvaite, and discusses some of the genesis of ilvaite.

A brief account of geology in the Asama area has been given by Nakamura (1971). The igneous petrology of the Asama complex has been investigated by Agata (1989, 1994), who has shown that the complex had a parental magma of a Hawaiian tholeiite composition and formed in an oceanic island.

Geological background

The Asama igneous complex has an exposed area of about 500 × 6000 m (Agata, 1989, 1994). Its margins terminate against basaltic rocks by faults, and there is no trace of chilled rocks. The layered structures, including modal layering and igneous

Mineralogical Magazine, September 1995, Vol. 59, pp. 489–496

lamination, are nearly vertical and generally strike E-W. The layered sequence comprises dunite, plagioclase wehrlite, olivine gabbro, anorthositic gabbro and two-pyroxene gabbro. The complex is divided into three zones: (1) the Lower zone consisting mainly of peridotites (about 200 m thick); (2) the Middle zone comprising a sequence of alternating peridotites and gabbros (about 200 m thick); and (3) the Upper zone composed mainly of gabbroic rocks (about 60 m thick). The crystallisation sequence of cumulus minerals is olivine and chromite first, followed by clinopyroxene and plagioclase together, and the final appearance of orthopyroxene. Olivine decreases its Fo mole from 89 to 78% from the base to the middle portion of the exposed layered sequence. The composition of clinopyroxene varies from $Ca_{49}Mg_{46}Fe_5$ to $Ca_{40}Mg_{47}Fe_{13}$ with the stratigraphic height.

The Mikabu greenstone belt, in which the Asama igneous complex occurs, underwent the Sambagawa regional metamorphism of pumpellyite–actinolite to greenschist facies (e.g. Seki *et al.*, 1964; Banno, 1992;). Secondary minerals such as albite, pumpellyite, actinolite and chlorite are widespread in the Asama complex. These secondary minerals are apparently products of the Sambagawa metamorphism. Pumpellyite and albite replaced magmatic plagioclase. Small amounts of clinozoisite and grossular are locally associated with pumpellyite and albite. Actinolite replaced magmatic clinopyroxene. Chlorite was observed in the contacts between olivine and albite–pumpellyite mixture after magmatic plagioclase.

The Asama peridotites underwent serpentinization in addition to the Sambagawa metamorphism. Most olivine grains were converted to aggregates of chrysotile and associated minerals, some of which also replaced actinolite, pumpellyite and some other minerals that are products of the Sambagawa metamorphism. Serpentine usually occurs together with secondary clinopyroxene and magnetite. Secondary clinopyroxene is generally fibrous and in places prismatic. Fibrous clinopyroxene commonly forms radial aggregates together with serpentine. Prismatic clinopyroxene is generally disseminated in aggregates of serpentine, and in places replaced actinolite. Prismatic clinopyroxene also forms network veinlets, which commonly contain chlorite,

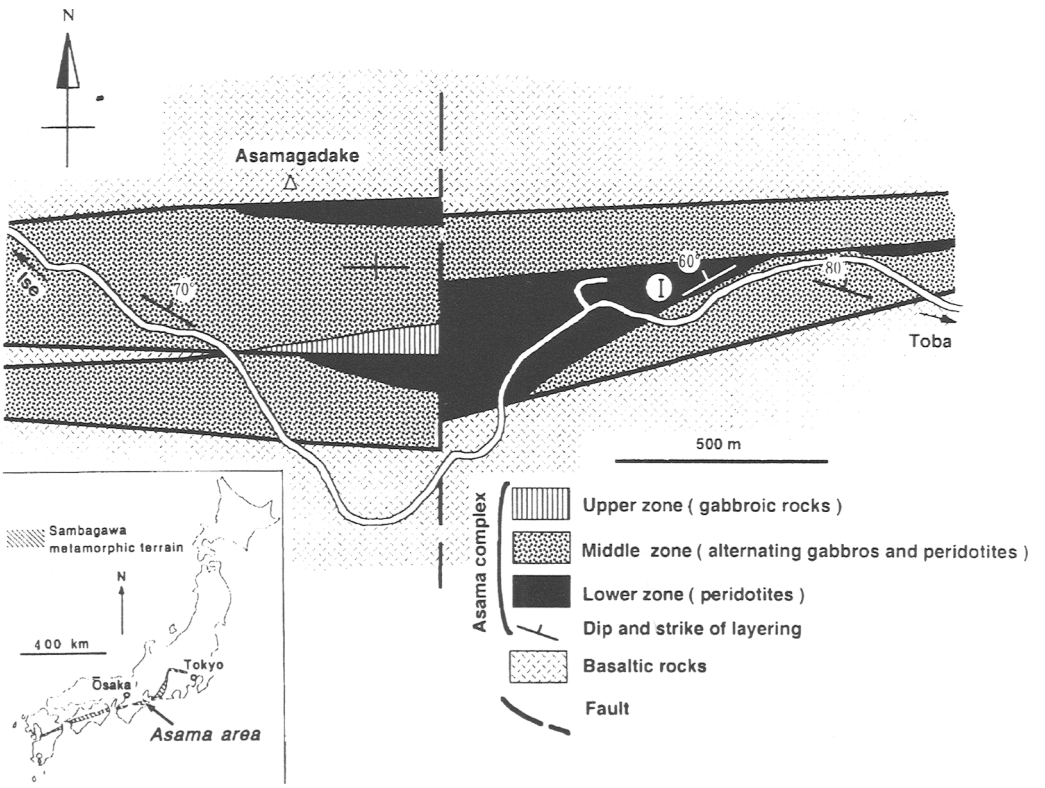

FIG. 1. Geological map of the Asama area, showing the locality of ilvaite (I).

locally andradite and rarely melanite. Clinopyroxene veinlets cut both igneous and metamorphic minerals including actinolite, albite and pumpellyite. Clinopyroxene is a rather rare mineral as a product during serpentinization, but has been sometimes reported in serpentinites of the Mikabu greenstone belt (e.g. Onuki *et al.*, 1982; Mouri and Enami, 1988). Magnetite is disseminated in mats of serpentine and fibrous clinopyroxene. 'Ferritchromit' (Fe^{3+}-rich Cr spinel formed as the result of alteration of magmatic chromite; Ramdohr, 1969) occurs in rims of igneous chromite. The amount of 'Ferritchromit' increases with increasing amounts of serpentine; 'Ferritchromit' presumably formed during the serpentinization.

Occurrence

Ilvaite was found in only one serpentinized plagioclase wehrlite sample (sample no. = MA-1) that occurs at the top of the Lower zone (Fig. 1). The ilvaite-bearing plagioclase wehrlite is an olivine–chromite heteradcumulate.

Cumulus olivine (Fo_{82}) and chromite show euhedral to subhedral grains enveloped by poikilitic intercumulus clinopyroxene ($Ca_{48}Mg_{45}Fe_7$–$Ca_{48}Mg_{43}Fe_9$) and plagioclase. Chromite usually forms discrete grains and occasionally intergrowths with ilmenite. The minerals formed as the result of the Sambagawa metamorphism comprise albite, pumpellyite, grossular, clinozoisite, chlorite and actinolite.Ilvaite is sparsely disseminated in mats of chrysotile and fibrous clinopyroxene that replaced olivine. It shows generally prismatic, and in places irregular, grains smaller than 0.2 mm in size, and locally forms aggregates of several grains. A strong pleochroism was observed in ilvaite: X = light brown, Y = dark brown, and Z = dark green.

The minerals associated with ilvaite comprise magnetite and andradite. They generally form irregular, anhedral grains. Disseminated prismatic clinopyroxene is also associated with ilvaite. The other secondary minerals in the ilvaite-bearing sample include 'Ferritchromit' intergrown with ilmenite. The 'Ferritchromit'–ilmenite intergrowth forms rims of chromite–ilmenite intergrowth. The intergrown 'Ferritchromit' and ilmenite are probably alteration products of ilmenite–chromite intergrowth that presumably formed as the result of exsolution of Ti-rich chromite before the formation of 'Ferritchromit' (Agata, 1994).

X-ray crystallography and chemistry

Ilvaite was examined on a Rigaku RU-200 X-ray microdiffractometer, using V-filtered Cr-$K\alpha$ radiation; accelerating voltage 50 kV, current 200 mA. Nineteen X-ray diffraction peaks were obtained from four selected ilvaite polygrain areas about 30 μm in diameter, and the diffraction pattern is roughly similar to that in Powder Diffraction File, Set 11–15 (1972).

Two polymorphs of ilvaite have been recognized by Bartholomè *et al.* (1968) and Dietrich (1972): orthorhombic and monoclinic polymorphs. The monoclinic β angle of ilvaite is related to the occupancies of Fe^{2+} and Fe^{3+} in the Fe(11) and Fe(12) sites (Takèuchi *et al.*, 1983) and changes from 90.00° (orthorhombic) to 90.61° with increasing Fe^{2+}–Fe^{3+} order parameter (η = |OP−50|/50, where OP is atomic % occupancy of Fe^{2+} or Fe^{3+} in one of the two sites) (Finger and Hazen, 1987). A lattice constant determination of the Asama ilvaite with monoclinic constraints, by a least-squares refinement of 15 selected peaks that overlap no other peaks, gives the β angle of 90.19(4)°. The determined β angle deviates by more than 4.7σ from 90°; the diffraction pattern, moreover, showed *hkl*–*hk*$\bar{l}$ peak splitting that is characteristic of monoclinic ilvaite (Dietrich, 1972).

The Asama ilvaite is probably monoclinic; its order parameter was calculated to be 0.31 by using the equation of Finger and Hazen (1987). The unit cell parameters except for the β angle are: a = 13.019(5), b = 8.808(2), and c = 5.850(4) Å.

Ilvaite and other minerals were analysed on a JEOL electron probe X-ray microanalyser, Model JCXA-733. Accelerating voltage, specimen current and beam diameter were 15 kV, 1.2–1.3 × 10^{-8} A and 3 μm, respectively.

Representative electron microprobe analyses of ilvaite are given in Table 1. The composition of ilvaite is close to the ideal end-member composition ($CaFe_2^{2+}Fe^{3+}Si_2O_8(OH)$). Ilvaite also contains 1.7–2.2 wt.% MgO and 1.9–2.5 wt.% MnO. The composition of secondary clinopyroxene lies close to the join diopside–hedenbergite (Table 2). Clinopyroxene associated with ilvaite has compositions around $Ca_{47}Mg_{45}Fe_8$ (Fig. 2). 'Ferritchromit' intergrown with ilmenite is enriched in Ti, Fe^{3+} and Fe^{2+}, when compared to chromite core intergrown with ilmenite (Table 3).

Discussion

The associated minerals suggest that ilvaite in the Asama complex formed during serpentinization. Secondary minerals associated with serpentine in places replaced albite, pumpellyite, actinolite and some other minerals that are apparently products of the Sambagawa metamorphism; the formation of ilvaite probably did not take place before the Sambagawa metamorphism. There is no evidence suggesting that any thermal events occurred after the

Sambagawa metamorphism was complete. The serpentinization related to the formation of ilvaite might have been an alteration that accompanied the Sambagawa metamorphism.

The Asama ilvaite-bearing assemblage, whose minerals are in contact with one another, is serpentine–clinopyroxene–ilvaite–andradite–magnetite. The ilvaite-free mineral assemblage that formed during the serpentinization is usually serpentine–clinopyroxene–magnetite. The assemblage serpentine–clinopyroxene–ilvaite–andradite–magnetite is invariant at a fixed T and P in the system Ca–Mg–Fe–Si–O–H with a fluid containing H_2O and O_2. The chemical reactions expressing the equilibrium relations between the minerals of the invariant assemblage may include:

$$\underset{\text{hedenbergite}}{6CaFeSi_2O_6} + \underset{\text{magnetite}}{4Fe_3O_4} + 3H_2O = \underset{\text{ilvaite}}{6CaFe_3Si_2O_8(OH)} + \tfrac{1}{2}O_2 \quad (1)$$

$$\underset{\text{hedenbergite}}{26CaFeSi_2O_6} + \underset{\text{andradite}}{8Ca_3Fe_2Si_3O_{12}} + \underset{\text{serpentine}}{12Mg_3Si_2O_5(OH)_4} = \underset{\text{ilvaite}}{14CaFe_3Si_2O_8(OH)} + \underset{\text{diopside}}{36CaMgSi_2O_6} + 17H_2O + \tfrac{1}{2}O_2 \quad (2)$$

$$\underset{\text{diopside}}{27CaMgSi_2O_6} + \underset{\text{magnetite}}{7Fe_3O_4} + 18H_2O = \underset{\text{serpentine}}{9Mg_3Si_2O_5(OH)_4} + \underset{\text{andradite}}{6Ca_3Fe_2Si_3O_{12}} + \underset{\text{hedenbergite}}{9CaFeSi_2O_6} + \tfrac{1}{2}O_2 \quad (3)$$

The phase relations between ilvaite, magnetite and andradite at a fixed T, P and P_{H_2O}, expected from these three chemical equations by assuming serpentine and clinopyroxene to be excess phases, can be depicted in the f_{O_2}–X_{di} (mole fraction of diopside) diagram as in Fig. 3. Figure 3 shows that the stability fields of ilvaite and andradite lie in relatively f_{O_2}-low portions; magnetite is stable in a portion of relatively high f_{O_2}. The Asama ilvaite-bearing assemblage occurs close to the assemblage serpentine–clinopyroxene–magnetite; the temperatures, pressures and water pressures during the formations of the two assemblages seem to have been similar to each other. The ilvaite-bearing assemblage lies at the invariant point in Fig. 3, and is considered to have formed at an f_{O_2} that was lower than that during the formation of the assemblage serpentine–clinopyroxene–magnetite.

A spinel–ilmenite geothermo- and oxygen geobarometer has been investigated by many authors (e.g. Buddington and Linsley, 1964; Powell and Powell, 1977). This geothermo- and oxygen geobarometer has been re-evaluated in the system Fe–Ti–O by Spencer and Linsley (1981), and Stormer (1983) has devised a method of calculation of temperature and oxygen fugacity for pairs of natural spinel and ilmenite containing MgO, Cr_2O_3 and some other elements. A grain of 'Ferritchromit'–ilmenite intergrowth occurs about 1 mm away from ilvaite grains.

TABLE 1. Representative electron microprobe analyses of ilvaite

	1	2	3	Theoretical
Sample no.	MA-1	MA-1	MA-1	
SiO_2	29.77	29.71	29.88	29.40
TiO_2	0.00	0.09	0.03	–
Al_2O_3	0.04	0.04	0.02	–
Fe_2O_3*	20.11	19.35	19.73	19.53
FeO	29.91	30.58	29.80	35.15
MnO	2.19	1.91	2.43	–
MgO	1.95	1.75	2.16	–
CaO	13.94	13.82	13.66	13.72
Total	97.91	97.25	97.71	97.80
Cation ratios on the basis of O = 8.5				
Si	1.992	2.003	2.001	2.000
Al	0.003	0.003	0.002	–
Ti	0.000	0.005	0.002	–
Fe^{3+}	1.013	0.982	0.994	1.000
Fe^{2+}	1.674	1.724	1.669	2.000
Mn	0.124	0.109	0.138	–
Mg	0.195	0.176	0.216	–
Ca	0.999	0.998	0.980	1.000

* Calculated with adjustment of total cations to 6 for O = 8.5.

TABLE 2. Representative electron microprobe analyses of clinopyroxene, garnet, magnetite, serpentine and chlorite

Sample no.	1 MA-1	2 TO-8	3 TB-2	4 MA-1	5 MA-1	6 MA-1	7 MA-1	8 TB-1	9 MA-1	10 TB-1
Mineral	Cpx	Cpx	Cpx	Cpx	And	Mela	Mt	Mt	Chry	Chl
SiO_2	54.20	54.58	54.04	53.02	35.90	32.08	1.03	0.71	42.89	29.61
TiO_2	0.10	0.00	0.00	0.13	0.20	12.25	0.11	0.17	0.01	0.00
Al_2O_3	0.19	0.18	0.44	0.28	0.96	0.72	0.00	0.00	0.05	17.52
Cr_2O_3	0.02	0.00	0.13	0.00	0.00	0.00	0.00	0.00	0.00	0.00
Fe_2O_3	–	–	–	–	29.17[t]	20.55[t]	66.07*	67.17*	–	–
FeO	4.99[tt]	2.72[tt]	6.50[tt]	11.07[tt]	–	–	32.12	32.06	1.85[tt]	17.38[tt]
MnO	0.17	0.16	0.52	0.45	0.07	0.10	0.09	0.00	0.01	0.24
MgO	16.45	18.07	14.77	11.34	0.17	0.58	0.00	0.06	41.87	23.45
NiO	0.00	0.00	0.00	0.00	0.00	0.00	0.00	0.00	0.00	0.07
CaO	23.12	23.50	23.00	24.01	33.25	33.68	0.14	0.04	0.08	0.06
Na_2O	0.11	0.13	0.21	0.11	–	–	–	–	0.02	0.00
K_2O	0.00	0.00	0.00	0.00	–	–	–	–	0.01	0.00
Total	99.35	99.34	99.61	100.41	99.72	99.96	99.56	100.21	86.79	88.33
					Cation ratios					
O≡	6	6	6	6	12	12	4	4	7	14
Si	2.000	1.995	2.004	1.999	3.020	2.672	0.004	0.027	2.002	2.957
Al	0.008	0.008	0.019	0.013	0.096	0.071	0.000	0.000	0.003	2.074
Ti	0.003	0.000	0.000	0.004	0.013	0.767	0.003	0.005	0.000	0.000
Cr	0.001	0.000	0.004	0.000	0.000	0.000	0.000	0.000	0.000	0.000
Fe^{3+}	–	–	–	–	1.846	1.288	1.914	1.936	–	–
Fe^{2+}	0.154	0.083	0.202	0.349	–	–	1.034	1.027	0.072	1.452
Mn	0.005	0.005	0.016	0.014	0.005	0.007	0.003	0.000	0.000	0.020
Mg	0.905	0.985	0.817	0.638	0.021	0.072	0.000	0.003	2.913	3.491
Ni	0.000	0.000	0.000	0.000	0.000	0.000	0.000	0.000	0.000	0.005
Ca	0.914	0.985	0.914	0.970	2.996	3.005	0.006	0.002	0.004	0.007
Na	0.008	0.009	0.015	0.008	–	–	–	–	0.002	0.000
K	0.000	0.000	0.000	0.000	–	–	–	–	0.001	0.000

[t] Total iron as Fe_2O_3.
[tt] Total iron as FeO.
* Calculated from stoichiometry.
Cpx: clinopyroxene; And: andradite; Mela: melanite; Mt: magnetite; Chry: chrysotile; Chl: chlorite. 1, 5, 7 and 9: clinopyroxene–serpentine–ilvaite–andradite–magnetite; 2, 3 and 8: clinopyroxene–serpentine–magnetite; 4, 6 and 10: clinopyroxene veinlets. All the samples (rocks names: serpentinized plagioclase wehrlites) were collected from the ilvaite locality (Fig. 1).

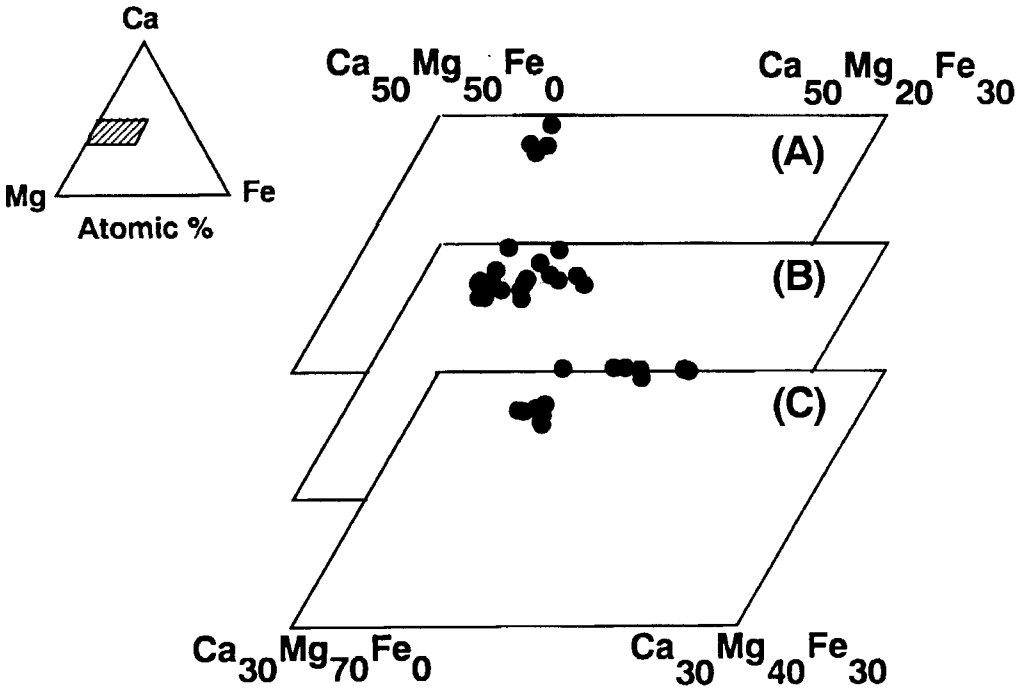

FIG. 2. Plots of secondary clinopyroxene on the Ca–Mg–Fe diagram. A: disseminated clinopyroxene associated with ilvaite, andradite, magnetite and serpentine; B: disseminated clinopyroxene associated with magnetite and serpentine (without ilvaite and andradite); C: clinopyroxene-forming veinlets.

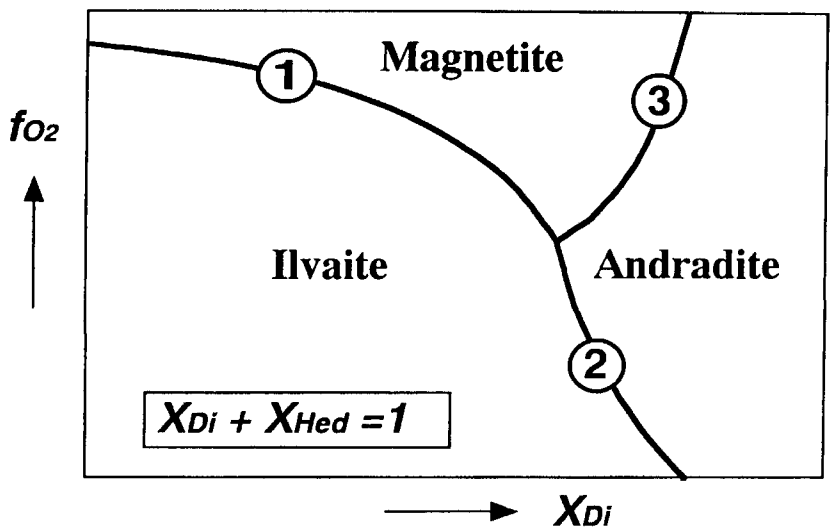

FIG. 3. Schematic stability fields of ilvaite, magnetite and andradite in the f_{O_2}-X_{di} diagram. Serpentine and clinopyroxene are excess phases; temperature, pressure and water pressure are fixed. Phase boundaries 1, 2 and 3, respectively, were inferred from chemical reactions 1, 2 and 3 in text by assuming $X_{di} + X_{hed} = 1$. X_{di} and X_{hed}: mole fractions of diopside and hedenbergite of clinopyroxene, respectively.

TABLE 3. Representative electron microprobe analyses of intergrown spinel and ilmenite in the ilvaite-bearing sample (MA-1)

	Spinel		Ilmenite	
	Rim	Core	Rim	Core
SiO_2	0.07	0.03	0.03	0.05
TiO_2	5.24	1.02	53.38	51.21
Al_2O_3	5.41	12.80	0.03	0.03
Cr_2O_3	9.37	27.02	0.19	0.27
Fe_2O_3*	43.07	27.69	0.45	5.44
FeO	34.32	23.69	41.94	37.44
MnO	0.42	0.31	0.86	0.57
MgO	1.25	6.73	2.87	4.54
NiO	0.21	0.18	0.11	0.00
CaO	0.03	0.00	0.00	0.00
Total	99.39	99.47	99.86	99.55
	Cation ratios			
O≡	4	4	3	3
Si	0.003	0.001	0.001	0.001
Ti	0.145	0.026	0.993	0.945
Al	0.236	0.513	0.001	0.001
Cr	0.273	0.725	0.004	0.005
Fe^{3+}	1.195	0.708	0.008	0.100
Fe^{2+}	1.059	0.673	0.867	0.769
Mn	0.013	0.009	0.018	0.012
Mg	0.069	0.341	0.106	0.166
Ni	0.006	0.005	0.002	0.000
Ca	0.001	0.000	0.000	0.000

* Calculated from stoichiometry

The 'Ferritchromit' were presumably equilibrated with the ilmenite at T and f_{O_2} that were similar to those of the formation of ilvaite. Using the calculation method of Stormer (1983), the 'Ferritchromit'–ilmenite equilibration temperature and oxygen fugacity were calculated to be 360–440°C and 10^{-31}–10^{-38}, respectively. The calculated temperatures and oxygen fugacities are concordant with those of the ilvaite synthesis investigated by Gustafson (1974).

The phase relations and calculated oxygen fugacities suggest that the Asama ilvaite formed under reducing conditions. Ramdohr (1967) has discovered native Fe in serpentinites and proposed that hydrogen gas was generated as the result of serpentinization of olivine. The presence of abundant hydrogen gas in fluid emanating from serpentinized peridotites has been reported by many authors (e.g. Neal and Stranger, 1983; Conveney *et al.*, 1987). The reducing conditions during the ilvaite formation in the Asama complex were presumably brought about by hydrogen gas that was generated as the result of the serpentinization of olivine.

Acknowledgements

We thank K. Suzuki of Nagoya University, who critically read the manuscript. We also acknowledge T. Kondo of Nagoya University, who kindly assisted us in the operation of the microdiffractometer. Thanks are due also to K. Shibata of Nagoya University for his discussion and encouragement. The work was supported partly by a Grant-in-Aid for Scientific Research from the Ministry of Education of Japan.

References

Agata, T. (1989) Asama layered igneous complex, Mikabu greenstone belt, central Japan. *DELP (Dynamics and Evolution of Lithosphere Project) Pub.* **28**, 83–4.

Agata, T. (1994) The Asama igneous complex, central Japan: an Ultramafic-mafic layered intrusion in the Mikabu greenstone belt, Sambagwa metamorphic terrain, central Japan. *Lithos*, **33**, 241–63.

Banno, Y. (1992) Blueschists in serpentinite conglomerates associated with the Mikabu greenstones in eastern Kii peninsula, Japan. *J. Petrol. Mineral. Econ. Geol.*, **87**, 207–20 (Japanese with English abstract).

Bartholomè, P., Duchesne, J.C. and Plas, L. (1968) Sur une forme monoclinique de l'ilvaite. *Ann. Soc. Geol. Belgique*, **90**, 779–88.

Barton, M. and Bergen, M.J. (1984) Secondary ilvaite in a dolerite dyke from Rogaland, SW Norway. *Mineral. Mag.*, **48**, 449–56.

Buddington, A.F. and Linsley, D.H. (1964) Iron–titanium oxide minerals and synthetic equivalents. *J. Petrol.*, **5**, 310–57.

Burt, D.M. (1971) The facies of some Ca–Fe–Si skarns in Japan. *Carnegie Inst. Washington Yearb.*, **70**, 185–8.

Conveney, R.M. Jr., Goebel, E.D., Zeller, E.J., Dreschhoff, G.A.M. and Angino, E.E. (1987) Serpentinization and the origin of hydrogen gas in Kansas. *A.A.P.G. Bull.*, **71**, 39–48.

Dietrich, V. (1972) Ilvait, Ferroantigorit und Greenalith als Begleter oxidisch-sulgidischer Vererzungen in den Oberhalbsteiner Serpentiniten. *Schweiz. Mineral. Petrogr. Mitt.*, **52**, 57–74.

Finger, L.W. and Hazen, R.M. (1987) Crystal structure of monoclinic ilvaite and the nature of the monoclinic-orthorhombic transition at high pressure. *Zeit. Krist.*, **179**, 415–30.

Graeser, S. (1975) Ilvait als alpines Zerrkluft-Mineral. *Schweiz. Mineral. Petrogr. Mitt.*, **55**, 1–7.

Gustafson, W.I. (1974) The stability of andradite,

hedenbergite, and related minerals in the system Ca–Fe–Si–O–H. *J. Petrol.*, **15**, 455–96.

Lucchetti, G. (1989) High-pressure ilvaite-bearing mineral assemblages from the Voltri group (Italy). *Neues Jahrb. Mineral. Mh.*, 1–7.

Mouri, K. and Enami, M. (1988) Chemical compositions of minerals from the Kichijosan and Joyama complexes in the Sanbagawa metamorphic belt, central Japan. *Bull. Nagoya Univ. Museum*, **4**, 15–30 (Japanese with English abstract).

Nakamura, Y. (1971) Petrology of the Toba ultrabasic complex, Mie Prefecture, central Japan. *J. Fac. Sci. Univ. Tokyo Ser. II*, **18**, 1–51.

Naslund, H.R., Hughes, M. and Birnie, R.W. (1983) Ilvaite, an alteration product replacing olivine in the Skaergaard intrusion. *Amer. Mineral.*, **68**, 1004–8.

Neal, C. and Stranger, G. (1983) Hydrogen generation from mantle source rocks in Oman. *Earth Planet. Sci. Lett.*, **66**, 315–20.

Onuki, H., Akasaka, M., Yoshida, T. and Nedachi, M. (1982) Ti-rich hydroandradites from the Sanbagawa metamorphic rocks of the Shibukawa area, central Japan. *Contrib. Mineral. Petrol.*, **80**, 183–8.

Powder Diffraction File, Set 11-15 (1972) Joint Committee on Powder Diffraction Standards.

Powell, R. and Powell, M. (1977) Geothermometry and oxygen barometry using coexisting iron-titan oxides: a reappraisal. *Mineral. Mag.*, **41**, 257–63.

Pesquera, A. and Velasco, F. (1986) An occurrence of ilvaite layers in the Cino Villas metasomatic rocks, western Pyrenees (Spain). *Mineral. Mag.*, **50**, 653–6.

Ramdohr, P. (1967) A widespread mineral association connected with serpentinization, with notes on some new or insufficiently defined minerals. *Neues. Jahrb. Mineral. Abh.*, **107**, 241–65.

Ramdohr, P. (1969) The Ore Mineral and their Intergrowths. Pergamon Press.

Seki, Y., Oba, T., Mori, R. and Kuriyagawa, S. (1964) Sambagawa metamorphism in the central part of Kii peninsula. *J. Japan. Assoc. Mineral. Petrol. Econ. Geol.*, **52**, 73–89 (in Japanese with English abstract).

Spencer, K.J. and Linsley, D.H. (1981) A solution model for coexisting iron-titanium oxides. *Amer. Mineral.*, **66**, 1189–201.

Stormer, J.C., Jr. (1983) The effect of recalculation on the estimates of temperature and oxygen fugacity from analyses of multicomponent iron-titanium oxides. *Amer.Mineral.*, **68**, 586–94.

Takèuchi, Y., Haga, N. and Bunno, M. (1983) X-ray study on polymorphism of ilvaite, $HCaFe_2^{2+}Fe^{3+}O_2[Si_2O_7]$. *Zeit. Krist.*, **163**, 267–83.

[*Manuscript received 18 August 1994: revised 28 October 1994*]